Numerical Heat Transfer, vol. 8, pp. 115–130, 1985

AN ALGORITHM TO REDUCE APPROXIMATION ERROR FROM THE COMPLEX-VARIABLE BOUNDARY-ELEMENT METHOD APPLIED TO SOIL FREEZING

T. V. Hromadka II
U.S. Geological Survey, Laguna Niguel, California 92667

G. L. Guymon
Department of Civil Engineering, University of California, Irvine, California 92717

An algorithm is presented for the numerical solution of the Laplace equation boundary-value problem, which is assumed to apply to soil freezing or thawing. The Laplace equation is numerically approximated by the complex-variable boundary-element method. The algorithm aids in reducing integrated relative error by providing a true measure of modeling error along the solution domain boundary. This measure of error can be used to select locations for adding, removing, or relocating nodal points on the boundary or to provide bounds for the integrated relative error of unknown nodal variable values along the boundary. Application of the algorithm to boundary-value problems is easily programmable and does not require extensive interpretation of modeling results.

INTRODUCTION

In a recent paper, Hromadka and Guymon [1] develop a geothermal numerical model based on a boundary integral equation method (BIEM). A major assumption in the model is that the phase change effects dominate the heat transfer conduction processes, and consequently the heat flux along the slow-moving freezing front (0°C isotherm) can be estimated by solving a Laplace equation in appropriately defined subregions. After heat flux values have been estimated along the freezing front, the front is spatially displaced according to the volumetric latent heat of fusion defined at the freezing front. In that paper, both a real-variable and a complex-variable BIEM numerical model are employed to solve the Laplace equation.

In this paper, the complex-variable BIEM will be used to develop an algorithm for obtaining a high level of accuracy in numerical results. This is important in problems where there is a need to estimate heat flux along the freezing front to some desired level of precision. Complex-variable methods are used because they provide a convenient measure of relative error, which is directly (and exactly) determined along the problem boundary. The algorithm utilizes the Cauchy integral model [2] to generate estimates for the values of unknown variables (state variable or stream function) along the boundary. These values are then used with another Cauchy integral model to generate values for comparison with the original boundary conditions. Comparison of these second estimates with the known boundary values gives an error distribution on the boundary, which is used to relocate or add nodal points for another model solution. In this fashion,

NOMENCLATURE

i^2	-1	ξ_u	unknown nodal value
N_k	basis function	ξ_u, ϵ_k	unknown and known nodal values
s	local coordinate		estimates from $\hat{\omega}$
x, y	coordinates	ϕ_j, ψ_j	nodal values of ϕ, ψ
z	$x + iy$	$\hat{\omega}$	CVBEM approximation
z_j	nodal coordinate	$\hat{\omega}_j$	nodal value of $\hat{\omega}(z_j)$
Γ	boundary	$\omega(z)$	complex analytic function
ξ_k	known nodal value	Ω	domain

the model is used to develop approximations for the unknown boundary variables and also evaluate the modeling error characteristics.

This paper addresses only the error reduction algorithm and its application in reducing the modeling relative error developed along the problem boundary for typical large-scale geothermal problems such as those involving roadway embankments. Consequently, the model applications are focused on steady-state solution (Laplace equation) problems.

By using the algorithm, the complex-variable geothermal model of Hromadka and Guymon [1] can be directly extended to provide a two-dimensional moving boundary geothermal model where phase change latent heat effects dominate the thermal regime.

THE COMPLEX-VARIABLE BOUNDARY-ELEMENT METHOD

In this section, a brief review of the complex-variable boundary-element method (CVBEM) is presented; a detailed development is given in [2].

A complex-variable analytic function $\omega(z)$ is composed of two real-variable two-dimensional functions

$$\omega(z) = \phi(x, y) + i\psi(x, y) \qquad z \in \Omega \tag{1}$$

where $z = x + iy$, $i = \sqrt{-1}$, $\phi(x, y)$ is a potential function, and $\psi(x, y)$ is a stream function. In Eq. (1), $\omega(z)$ is defined only in a simply connected domain Ω in which $\omega(z)$ is analytic [3]. The conjugate functions composing $\omega(z)$ are related by the Cauchy-Riemann equations

$$\frac{\partial \phi}{\partial x} = \frac{\partial \psi}{\partial y} \qquad \frac{\partial \phi}{\partial y} = -\frac{\partial \psi}{\partial x} \tag{2}$$

Consequently, each function is harmonic and

$$\frac{\partial^2 \xi}{\partial x^2} + \frac{\partial^2 \xi}{\partial y^2} = 0 \qquad z \in \Omega \qquad \xi = \phi, \psi \tag{3}$$

For an analytic function $\omega(z)$ defined in domain Ω and on boundary Γ (Fig. 1), Cauchy's integral theorem equates the value of $\omega(z_0)$ to a boundary integral on Γ with

$$2\pi i \omega(z_0) = \oint_\Gamma \frac{\omega(z)\, dz}{z - z_0} \tag{4}$$

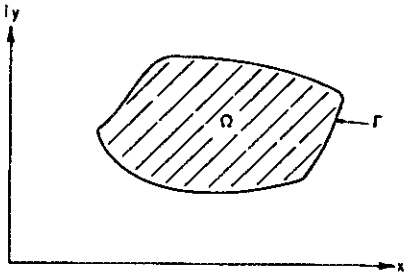

Fig. 1 Problem domain Ω with boundary contour Γ.

where z_0 is the interior of Ω and the line integral is in the positive sense (Fig. 2). From Eq. (4), a BIEM can be developed which is analogous to real-variable BIEM models. As in the real-variable BIEM models, the global boundary Γ is subdivided into boundary elements by boundary nodal points.

For a point z_0 in the interior of Ω, the Cauchy integral can be rewritten as the sum of m line integrals (for m CVBE)

$$2\pi i\omega(z_0) = \sum_{j=1}^{m} \int_{\Gamma_j} \frac{\omega(z)\,dz}{z - z_0} \tag{5}$$

where Γ_j is a complex-variable boundary element (CVBE) in an m-element model (Fig. 3). On each Γ_j, n nodal points $(z_1, z_2, \ldots, z_n)$ are located as shown in Fig. 4. To define a linear local coordinate system (Fig. 5), the following relations can be used to calculate the CVBE Γ_j contribution to the line integral of Eq. (5):

$$\left.\begin{aligned} z(s) &= z_1 + (z_n - z_1)s \\ dz &= (z_n - z_1)\,ds \\ \omega(z) &= \omega(z(s)) \end{aligned}\right\} \quad z \in \Gamma_j \qquad 0 \leqslant s \leqslant 1 \tag{6}$$

where s is a local coordinate.

In the following, the notation $\omega(s)$ will be used for the $\omega_j(z(s))$ function on each Γ_j.

The Cauchy boundary integral can be written as the sum of m CVBE contributions

$$2\pi i\omega(z_0) = \sum_{j=1}^{m} \left[\int_{s=0}^{1} \frac{\omega_j(s)(z_n - z_1)\,ds}{z(s) - z_0} \right]_j \tag{7}$$

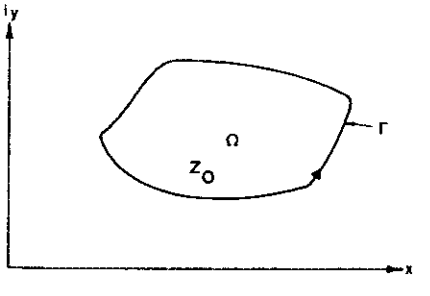

Fig. 2 Domain Ω with interior point z_0. The positive sense on the boundary Γ is shown by an arrowhead.

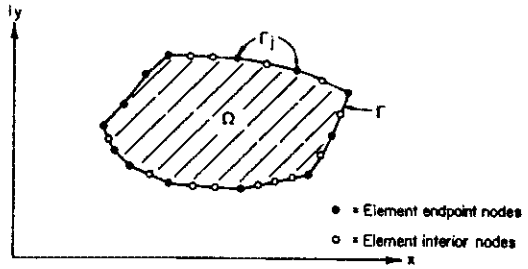

Fig. 3 Global domain Ω with global boundary Γ subdivided into boundary elements Γ_j.

where the $[\ ]_j$ notation indicates the value from CVBE Γ_j. Equation (7) can be simplified to

$$2\pi i\omega(z_0) = \sum_{j=1}^{m} \left[\int_{s=0}^{1} \frac{\omega_j(s)\,ds}{s + C_j} \right]_j \qquad 0 \leqslant s \leqslant 1 \tag{8}$$

where
$$C_j = \frac{z_1 - z_0}{z_n - z_1} \tag{9}$$

and
$$\omega_j(s) = \phi_j(s) + i\psi_j(s) \qquad 0 \leqslant s \leqslant 1 \tag{10}$$

Equation (8) can now be rewritten as a sum of definite integrals

$$\int_{s=0}^{1} \frac{\omega_j(s)\,ds}{s + C_j} = \int_{s=0}^{1} \frac{\phi_j(s)\,ds}{s + C_j} + i \int_{s=0}^{1} \frac{\psi_j(s)\,ds}{s + C_j} \tag{11}$$

The assumed approximation functions for $\phi(s)$ and $\psi(s)$ are now expressed by

$$\phi_j(s) \equiv \sum_{k=1}^{n} N_k(s)\phi_k \qquad 0 \leqslant s \leqslant 1 \tag{12}$$

$$\psi_j(s) \equiv \sum_{k=1}^{n} N_k(s)\psi_k \qquad 0 \leqslant s \leqslant 1 \tag{13}$$

The shape functions $N_k(s)$ are analogous to the one-dimensional interpolation functions used in finite-element methods [4], and (ϕ_k, ψ_k) indicate values of ϕ and ψ at nodal point k of CVBE Γ_j.

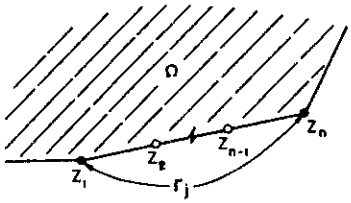

Fig. 4 Boundary element Γ_j with associated nodal points $z_1, \ldots, z_n$.

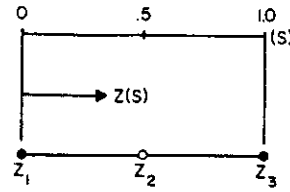

Fig. 5 Definition of the local coordinate system.

Combining Eqs. (5), (8), (12), and (13) gives the CVBEM approximation statement

$$2\pi i\hat{\omega}(z_0) = \sum_{j=1}^{m}\left(\int_{s=0}^{1}\frac{\Sigma N_k\phi_k\,ds}{s+C}\right)_j + i\sum_{j=1}^{m}\left(\int_{s=0}^{1}\frac{\Sigma N_k\psi_k\,ds}{s+C}\right)_j \tag{14}$$

APPLICATION OF THE CVBEM TO THE UNIT CIRCLE

In this section the CVBEM will be applied to the unit circle centered at the origin of the coordinate axis. The boundary Γ is assumed to be subdivided into m boundary elements Γ_j of equal length. The approximation used is the constant CVBEM, which includes a single node ζ_j centered on each Γ_j, and the nodal value $\hat{\omega}_j = \hat{\omega}(\zeta_j)$ is assumed to specify the function on Γ_j, i.e., $\hat{\omega}(z) = \hat{\omega}_j, z \in \Gamma_j$.

Figure 5 shows the assumed CVBEM configuration. The following definitions are used:

$$\Delta\theta = \frac{2\pi}{m}$$

$$\theta_1 = 2\pi - \frac{\pi}{m}$$

$$\theta_2 = \frac{\pi}{m}$$

$$\theta_3 = \frac{3\pi}{m}$$

$$\theta_k = \frac{2(k-2)\pi}{m} + \frac{\pi}{m}$$

Let $d(z_k, \zeta_1)$ = the distance from coordinate z_k to ζ_1. Then

$$d(z_k, \zeta_1) = 2\sin\frac{\theta_k}{2} \tag{15}$$

Using Cauchy's theorem, the limit of $\omega(z)$ can be used to evaluate

$$\omega_1 = \omega(\zeta_1) = \lim_{z^*\to\zeta_1}\frac{1}{2\pi i}\int_\Gamma\frac{\omega(z)\,dz}{z-z^*} \tag{16}$$

where z^* approaches nodal coordinate ζ_1 from the interior of Ω. Thus

$$2\pi i\omega_1 = \lim_{z^*\to\zeta_1} \sum_{j=1}^{m} \int_{\Gamma_j} \frac{\omega(z)\,dz}{z - z^*} \tag{17}$$

For the constant-boundary-element approximation, we set

$$\begin{aligned} 2\pi i\hat{\omega}_1 &= \lim_{z^*\to\zeta_1} \sum_{j=1}^{m} \hat{\omega}_j \int_{\Gamma_j} \frac{dz}{z - z^*} \\ &= \sum_{j=2}^{m} \hat{\omega}_j \ln\left(\frac{z_{k+1} - \zeta_1}{z_k - \zeta_1}\right) + \lim_{z^*\to\zeta_1} \left(\hat{\omega}_1 \int_{z_1}^{z_2} \frac{dz}{z - z^*}\right) \\ &= \sum_{j=2}^{m} \hat{\omega}_j \left\{ \ln\left[\frac{d(z_{k+1}, \zeta_1)}{d(z_k, \zeta_1)}\right] + i\left(\frac{\Delta\theta}{2}\right)\right\} + i\pi\left(1 + \frac{1}{m}\right)\hat{\omega}_1 \end{aligned} \tag{18}$$

Thus, the approximation used is

$$a_1\hat{\omega}_1 - a_2\hat{\omega}_2 - a_3\hat{\omega}_3 - a_m\hat{\omega}_m = 0 \tag{19}$$

where

$$a_1 = i\pi\left(1 - \frac{1}{m}\right)$$

$$a_k = \ln\left(\cos\frac{\Delta\theta}{2} + \sin\frac{\Delta\theta}{2}\cot\frac{\theta_k}{2}\right) + i\frac{\Delta\theta}{2}$$

For m large, $\Delta\theta$ is small, simplifying the real part of a_k to

$$a_k = \ln\left(1 + \frac{\Delta\theta}{2}\cot\frac{\theta_k}{2}\right) \tag{20}$$

where $\Delta\theta/2 = \pi/m$.

By symmetry, the nodal point ζ_1 could represent any nodal point ζ_j for $j = 1, 2, \ldots, m$. Thus, a matrix system is determined by

$$\begin{bmatrix} -a_1 & a_2 & a_3 \cdots a_{m-1} & a_m \\ a_m & -a_1 & a_2 \cdots a_{m-2} & a_{m-1} \\ a_{m-1} & a_m & -a_1 \quad a_{m-3} & a_{m-2} \\ \vdots & & & \vdots \\ a_2 & a_3 & a_4 \cdots a_m & -a_1 \end{bmatrix} \begin{Bmatrix} \hat{\omega}_1 \\ \hat{\omega}_2 \\ \hat{\omega}_3 \\ \vdots \\ \hat{\omega}_m \end{Bmatrix} = \mathbf{L} \tag{21}$$

or simply $\mathbf{a}\hat{\omega} = \mathbf{L}$, where $\mathbf{L}$ is a load vector and where it is understood that in Eq. (21) at least one nodal value $\omega(z_j)$ is known and consequently the equation has a unique solution not necessarily identically zero.

Relative magnitudes of the a_k with respect to a_1 are given by

$$|R_k| = \left| \frac{a_k}{a_1} \right| \qquad k = 1, 2, \ldots, m \tag{22}$$

The definitions of a_k and a_1,

$$\lim_{m \to \infty} |a_1| = \pi$$

and

$$\lim_{\substack{m \to \infty \\ \theta_k \to 0}} |a_k| = \ln 3 \qquad \lim_{\substack{m \to \infty \\ \theta_k \to 2\pi}} |a_k| = |\ln \tfrac{1}{3}| = \ln 3 \tag{23}$$

Thus, R_k has a maximum value of $(\ln 3)/\pi$.
Thus, The global matrix system can be written in terms of R_k as

$$\begin{bmatrix} -1 & R_2 & R_3 \cdots R_{m-1} & R_m \\ R_m & -1 & R_2 \cdots R_{m-2} & R_{m-1} \\ R_{m-1} & R_n & -1 \quad \cdots R_{m-3} & R_{m-2} \\ \vdots & & & \vdots \\ R_2 & R_3 & R_4 \cdots R_m & -1 \end{bmatrix} \begin{Bmatrix} \hat{\omega}_1 \\ \hat{\omega}_2 \\ \hat{\omega}_3 \\ \vdots \\ \hat{\omega}_m \end{Bmatrix} = \mathbf{L} \tag{24}$$

or simply $\mathbf{R}\hat{\omega} = \hat{\mathbf{L}}$, where $\hat{\mathbf{L}}$ is a modified load vector containing known boundary condition information and where again in Eq. (24) at least one nodal value $\hat{\omega}(z_j)$ is known and $\hat{\omega}$ is not necessarily identically zero.

The unit circle approximation can be used to show how the error in the approximation is manifested in the $\hat{\omega}_j$ values. From the above, it can be concluded that if the assumed trial functions are the actual solution to the boundary-value problem, then $\hat{\omega} = \omega$ on $\Gamma \cup \Omega$. Suppose that on Γ, m boundary elements Γ_j of equal length δ are specified, and on each Γ_j

$$\hat{\omega} = \Sigma N_k \hat{\omega}_k \qquad \hat{\omega}_k = \hat{\omega}(z_k) \qquad z_k \in \Gamma_j$$

Also suppose that the trial functions N_k solve the boundary-value problem on each Γ_j except for one element, say Γ_2, where

$$\omega = \Sigma (N_k + M_k)\hat{\omega}_k \qquad z \in \Gamma_2$$

Then two global matrix systems can be developed such that

$$\begin{aligned} (\mathbb{C}_1 + \mathbb{C}_2)\omega &= \mathbf{L} \\ \mathbb{C}_1 \hat{\omega} &= \mathbf{L} \end{aligned} \tag{25}$$

where $\mathbb{C}_1$ is the global matrix of complex coefficients determined by solving the CVBEM nodal statement with only the N_k trial functions defined on each $\Gamma_j, j = 1, 2, 3, \ldots, m$,

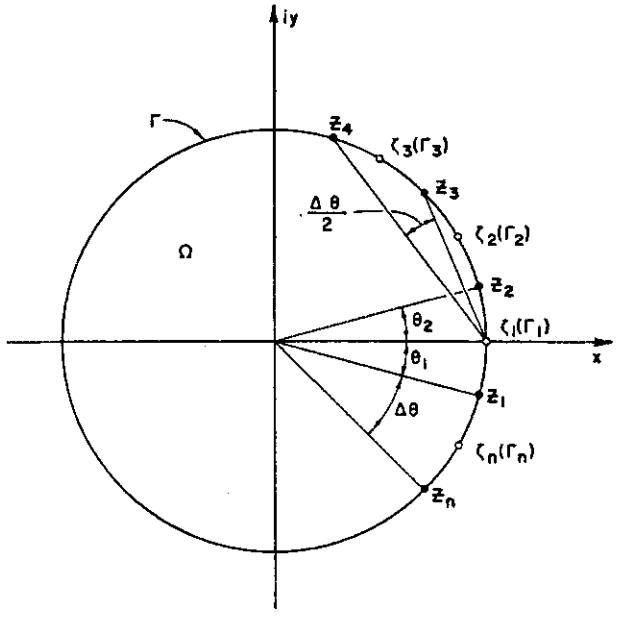

Fig. 6 Unit circle boundary-element geometry.

and $\mathbb{C}_2$ is a matrix of complex coefficients resulting from the M_k trial function contributions on element Γ_2. Note that ω are nodal values of the solution of the boundary-value problem, whereas $\hat{\omega}$ are approximations that differ from ω due to the incorrect trial functions assumed on Γ_2.

The CVBEM approximation $\hat{\omega}$ can be made arbitrarily close to ω by choosing the number of equally spaced nodal points m sufficiently large. The constant CVBEM assumes

$$\int_{\Gamma_j} \frac{\hat{\omega}\, dz}{z - z_0} = \hat{\omega}_j \int_{\Gamma_j} \frac{dz}{z - z_0}$$

and the approximation function $\hat{\omega}$ based on the sum of these contributions can be shown to be analytic. Due to constant trial function assumptions, a complex number k exists such that

$$\begin{aligned} &\int_{\Gamma_j} \frac{\omega\, dz}{z - z_0} = \omega_j \int_{\Gamma_j} \frac{dz}{z - z_0} \qquad j \neq 2 \\ &\int_{\Gamma_2} \frac{\omega\, dz}{z - z_0} = k\omega_2 \int_{\Gamma_2} \frac{dz}{z - z_0} \qquad \text{where } k = k(\delta) \end{aligned} \tag{26}$$

and $\delta = |\Gamma_j|$.

Then, from the previous development,

$$\mathbb{C}_1 = \mathrm{a}$$

and

$$\mathbb{C}_2 = k(\delta)\begin{bmatrix} 0 & a_2 & 0\cdots 0 \\ 0 & a_1 & 0\cdots 0 \\ \vdots & & \\ 0 & a_3 & 0\cdots 0 \end{bmatrix} \tag{27}$$

The error at each nodal point e_j is given by $\mathbf{e} = \omega - \hat{\omega}$, or

$$\mathbb{C}_1 \mathbf{e} = \mathbb{C}_2 \omega \tag{28}$$

where for the constant CVBEM with boundary elements of constant length δ

$$\mathbf{ae} = k(\delta)\omega_2(a_2, a_1, a_n, \ldots, a_3)^T \tag{29}$$

or

$$\mathbf{Re} = k(\delta)\omega_2(R_2, R_1, R_n, \ldots, R_3)^T$$

where $|R_1| = 1$ and $|R_j| < 0.35, j \neq 1$. Solving for $\mathbf{e}$ gives

$$\mathbf{e} = \begin{Bmatrix} 0 \\ k\omega_2 \\ 0 \\ \vdots \\ 0 \end{Bmatrix} \tag{30}$$

From the simple example above, it can be proposed that the nodal point approximation error will generally be manifested in the vicinity of the boundary element whose trial functions are incorrect. It can also be argued that the error of node 2 (element Γ_2) has the largest coefficient magnitude ($R_1 = 1$) and that the largest error contribution is assigned to node 2.

To improve the trial function and reduce integration errors, additional nodal points can be specified in the vicinity of the maximum relative error or, perhaps, the trial function order can be increased. In the next section, the results from the case above will be used to develop a CVBEM algorithm that addresses the approximation error on Γ, and ultimately in Ω.

A CVBEM ALGORITHM

In this section, the CVBEM is applied to the simple closed boundary Γ of domain Ω. Along Γ, values of ϕ or ψ are known continuously on piecewise segments. The solution of the Dirichlet boundary-value problem is the analytic function

$$\omega(z) = \Delta\xi_k + \Delta\xi_U \tag{31}$$

where the notation of Eq. (31) involves the descriptor

$$\Delta = \begin{cases} 1 & \text{if } \xi_x = \phi \quad x = k, U \\ i & \text{if } \xi_x = \psi \quad x = k, U \end{cases}$$

and ξ_k, ξ_U are the known and unknown harmonic functions of $\omega(z)$, respectively.

On Γ, we define m nodal points such that

$$\bar{\omega}_j = (\Delta\xi_k + \Delta\bar{\xi}_U)_j \quad j = 1, 2, \ldots, m \tag{32}$$

where each $\bar{\omega}_j$ is composed of a known boundary condition value ξ_k and an unknown nodal value $\bar{\xi}_U$.

The integration function $\hat{\omega}(z)$ is analytic in the interior of Γ, where

$$\hat{\omega}(z) = \frac{1}{2\pi i} \int_\Gamma \frac{\alpha(\zeta)\, d\zeta}{\zeta - z} \quad z \notin \Gamma \quad \zeta \in \Gamma \tag{33}$$

and where $\alpha(\zeta)$ are continuous functions on Γ. Because $\hat{\omega}(z)$ is analytic in the interior of Γ, we can define another boundary Γ^- that is an arbitrarily close measure of Γ and is interior to Γ. The boundary Γ^- is chosen such that $|\omega(z_1) - \omega(z_2)| < \epsilon$, where $\epsilon > 0$ and $z_1 \in \Gamma, z_2 \in \Gamma^-$. Using Γ^-,

$$\hat{\omega}(z) = \frac{1}{2\pi i} \int_{\Gamma^-} \frac{\hat{\omega}(z)\, d\zeta}{\zeta - z} \quad z \in \Gamma^- \text{ or } z \text{ interior to } \Gamma^- \tag{34}$$

For any z interior to Γ, we can choose an appropriate Γ^- such that Eq. (34) is valid and

$$\int_{\Gamma^-} \frac{\hat{\omega}(\zeta)\, d\zeta}{\zeta - z} = \int_\Gamma \frac{\alpha(\zeta)\, d\zeta}{\zeta - z} \tag{35}$$

The strategy in these definitions is to utilize a new boundary Γ^- arbitrarily close but interior to Γ such that $\omega(z)$ values are within ϵ between appropriate points on Γ and Γ^-. Then the approximation function defined along Γ^- is analytic on Γ^- and can be used to determine integrated error bounds. The error $e(z)$ is defined by the analytic function

$$e(z) = \omega(z) - \hat{\omega}(z) \quad z \in \Gamma^- \cup \Omega^- \tag{36}$$

where Ω^- is in the interior of Γ^-.

To evaluate Eq. (36), the $\omega(z)$ function must be determined. The algorithm defines $\omega(z)$ by using the definition of Eq. (33) and (34) and setting

$$\hat{\omega}(z_j) = (\Delta\hat{\xi}_k + \Delta\bar{\xi}_U)_j \quad j = 1, 2, \ldots, m \tag{37}$$

where z_j are nodal point coordinates. In Eq. (37) the integration function $\hat{\omega}(z)$ results in real and imaginary harmonic functions, where each function is itself a function of the nodal point values $\bar{\omega}_j$ defined by Eq. (32). If at node j the real state variable $\phi(z_j)$ is known as a boundary condition, then the imaginary equation for $\hat{\omega}(z_j)$ is used to solve for the unknown approximation $\Delta\bar{\xi}_U$. Likewise, if $\psi(z_j)$ is specified, then the real equation for $\hat{\omega}(z_j)$ is used to determine the unknown nodal value $\Delta\bar{\xi}_U$. Since $\hat{\omega}(z)$ is defined for $z \in \Omega^- \cup \Gamma^-$, the error function can be evaluated, where

$$e(z) = \Delta(\xi_k - \hat{\xi}_k) + \Delta(\xi_U - \hat{\xi}_U) \qquad z \in \Omega^- \cup \Gamma^- \tag{38}$$

In summary, the first step in the algorithm is to define the unknown nodal point values $(\Delta\bar{\xi}_U)_j$ such that the approximation function $\hat{\omega}(z)$ satisfies Eq. (37). Using the Cauchy integral formula on an arbitrarily close interior boundary Γ^-, $\hat{\omega}(z)$ is analytic on $\Gamma^- \cup \Omega^-$ and can be used to directly evaluate the error of approximation. To minimize the error, the relative error of $\Delta(\xi_k - \hat{\xi}_k)$ must also be minimized, so a calculation of $\Delta(\xi_k - \hat{\xi}_k)_j$ can be used to locate regions where nodal points should be added to reduce integration error due to the improved trial function assumptions. From the unit circle example of the previous section, relative error may be assumed to manifest itself in the vicinity of poor trial function fitting.

APPLICATIONS

Two example problems are presented to illustrate the use of the algorithm.

Example 1: Roadway Embankment Freezing

To model the freezing front, estimates of heat flux values are required along the 0°C isotherm, where a soil-water phase change occurs. In this example, a roadway embankment is modeled where the freezing front is assumed to be located about 10 m below the natural grade (Fig. 7). A −10°C boundary temperature is imposed along the entire top surface, and a 0°C temperature is specified along the bottom boundary at the freezing front. Symmetry is assumed on the left and right boundaries.

The CVBEM can be used to estimate values of the stream function ψ along the freezing front. From the Cauchy-Riemann relations, normal flux values of temperature (ϕ) are calculated.

Figures 7*b* and 7*c* show the continuous relative error distribution on Γ with two nodal densities, 26 and 32, where the 32-nodal model is based on one usage of the algorithm.

Example 2: Roadway Embankment Underlain by Buried Freezing Conduit

Another problem of interest is the analysis of soil-water freezing effects due to buried chilled pipelines or conduits. In this problem, the roadway geometry of example 1 is studied with a 1-m box conduit buried at a depth of 5 m (Fig. 8). The temperature of the conduit is set at −20°C. Figure 8*b* shows the relative error distribution on Γ for the first solution attempt with the CVBEM algorithm. Figure 8*c* shows the relative error distribution on Γ after four attempts using the algorithm.

Both example problems show that the relative error is significantly reduced by increasing the nodal point density in regions where relative error is manifested. In addition, the algorithm provides a means of obtaining a high level of accuracy in modeling estimates.

CONCLUSIONS

An algorithm for numerically solving a Dirichlet problem has been presented. The algorithm computes a true measure of integrated relative error along the solution

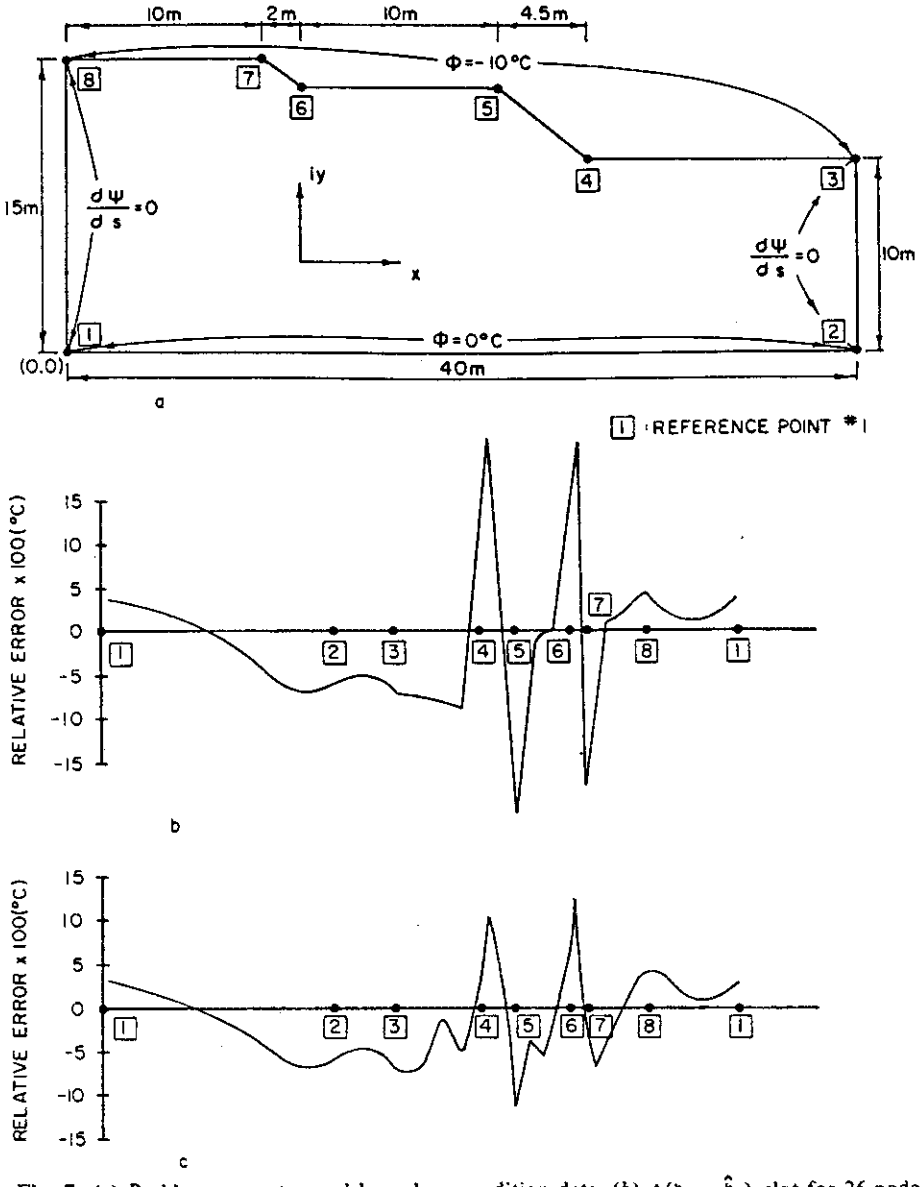

Fig. 7 (*a*) Problem geometry and boundary condition data. (*b*) $\Delta(\xi_k - \hat{\xi}_k)$ plot for 26-node model. (*c*) $\Delta(\xi_k - \hat{\xi}_k)$ plot for 32-node model.

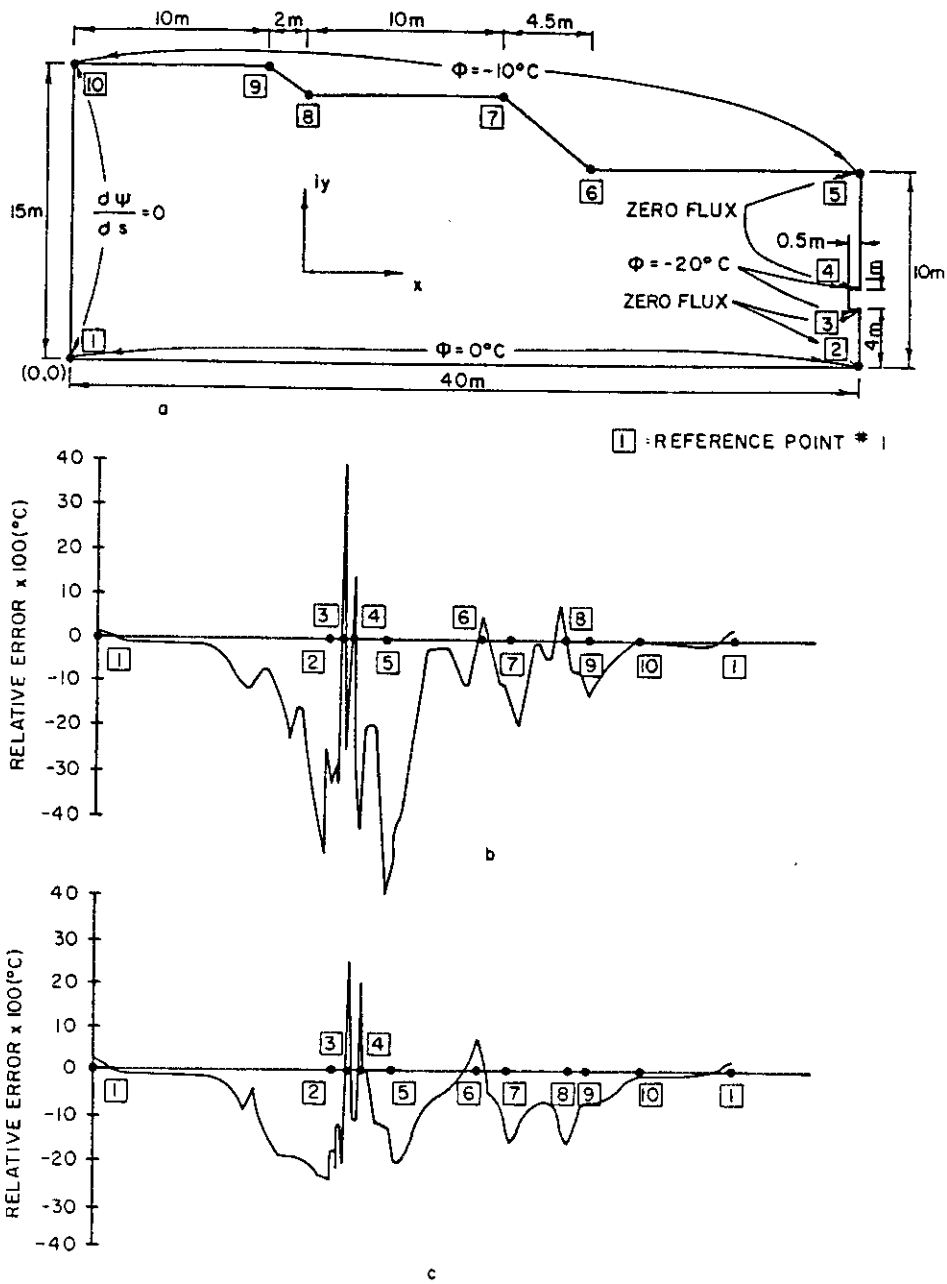

Fig. 8 (*a*) Problem geometry and boundary condition data. (*b*) $\Delta(\xi_k - \hat{\xi}_k)$ plot for 64-node model. (*c*) $\Delta(\xi_k - \hat{\xi}_k)$ plot for 76-node model.

domain boundary. The nodal point relative error values can be used to identify regions where a higher density of nodal points is needed to reduce the approximation error. In addition, the evaluation of computed error can indicate regions where nodal points can be eliminated without increasing the total error.

The algorithm is based on the complex-variable boundary-element method and is suitable for programming with both micro- and minicomputers.

APPENDIX

Rather than examine relative error values on the boundary Γ, it is useful to determine an approximative boundary $\hat{\Gamma}$ on which $\hat{\omega}(z)$ satisfies the boundary conditions given for $\omega(z)$ on $\hat{\Gamma}$. That is, given an approximator $\hat{\omega}(z)$, level curves of constant ϕ or ψ on Γ [where $\omega(z) = \phi + i\psi$ and $\hat{\omega}(z) = \hat{\phi} + i\hat{\psi}$] are compared with level curves of constant $\hat{\phi}$ or $\hat{\psi}$ on $\hat{\Gamma}$, where $\hat{\Gamma}$ is determined by setting the known $\phi = \hat{\phi}$ and $\psi = \hat{\psi}$.

The resulting boundary $\hat{\Gamma}$ has the associated property that $\hat{\omega}(z)$ satisfies the defined boundary conditions on $\hat{\Gamma}$ and satisfies the governing Laplace equation in the interior, $\hat{\Omega}$. Consequently, $\hat{\omega}(z)$ is the exact solution to the boundary-value problem with the true boundary Γ transformed to the approximative boundary $\hat{\Gamma}$.

Utilization of the approximative boundary has the following features:

1. An exact solution to the boundary-value problem is provided where the problem boundary is modified by a complex-variable transformation (which is undetermined).
2. The approximative boundary can be visually compared with the true boundary to determine closeness of geometric fit.
3. Nodal points can be added to Γ to give a more refined approximation $\hat{\omega}(z)$ so that $\hat{\Gamma}$ is closer to Γ in regions of high discrepancy.
4. The engineer works with a displacement of the problem boundary rather than examining a more abstract relative error propagation along the boundary.
5. The approximative boundary provides a direct visual representation of the sensitivity of the approximation $\hat{\omega}(z)$ in accommodating boundary conditions, variations in Γ geometry, and the addition of nodal points.

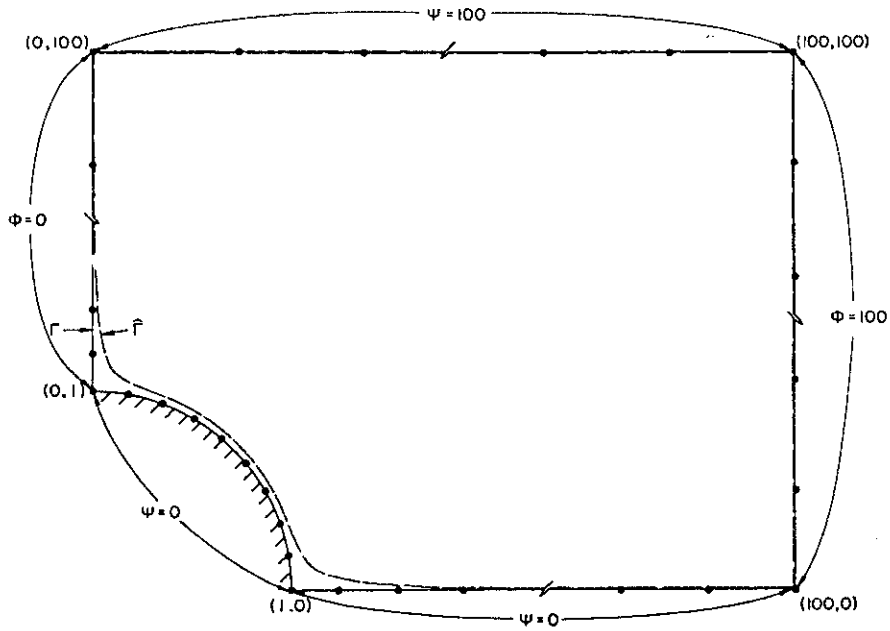

Fig. 9 Modeling ideal fluid flow over a cylinder.

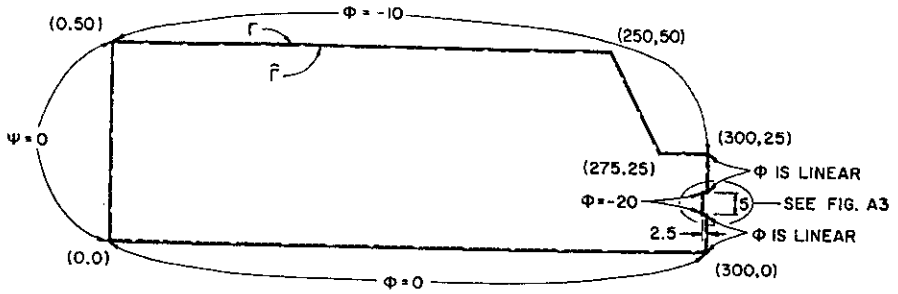

Fig. 10 Modeling the thermal effects of a freezing conduit in a roadway embankment.

Applications

In the following, several mixed boundary-value problems of the Laplace equation are approximated by the CVBEM. The problems all have boundaries Γ that geometrically coincide with lines of constant ϕ or ψ of $\omega(z)$. After an $\hat{\omega}(z)$ is developed, the approximative boundary $\hat{\Gamma}$ is determined by plotting the corresponding lines of constant $\hat{\phi} = \phi$ and $\hat{\psi} = \psi$ from $\hat{\omega}(z)$. In the figures, both Γ and the associated $\hat{\Gamma}$ are plotted together for direct comparison. Intuitively, as $\|\hat{\Gamma} - \Gamma\|$ becomes small then $|\hat{\omega}(z) - \omega(z)|$ is necessarily reduced, and $\|\hat{\Gamma} - \Gamma\| = 0$ implies $\hat{\omega}(z) = \omega(z)$.

Application 1. This problem approximates the classical problem of ideal fluid flow over a cylinder. The exact solution is known to be $\omega(z) = z + 1/z$. The problem boundary Γ is specified to be the upper right quadrant as shown in Fig. 9. Using a 47-node discretization, $\hat{\omega}(z)$ is developed by using the CVBEM. The corresponding approximative boundary $\hat{\Gamma}$ is plotted along with the true boundary Γ in Fig. 9.

Application 2. The usefulness of the CVBEM and the approximative boundary concept is illustrated for practical problems where the true solution $\omega(z)$ is unknown.

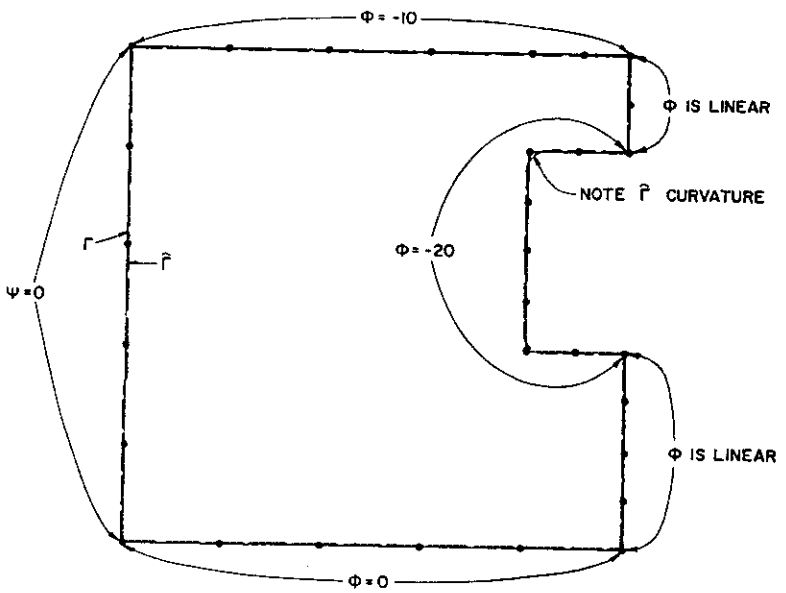

Fig. 11 The approximate boundary near the freezing conduit (square-shaped).

Using only the known boundary conditions, $\hat{\omega}(z)$ is determined. In Fig. 10, a large roadway embankment is modeled for heat transfer effects. A freezing conduit is defined on the right side of the boundary. The approximative boundary $\hat{\Gamma}$ corresponding to a 78-node $\hat{\omega}(z)$ approximation is shown in Fig. 10. A closer look at $\hat{\Gamma}$ and Γ near the conduit is provided in Fig. 11.

REFERENCES

1. T. V. Hromadka II and G. L. Guymon, Applications of a Boundary Integral Equation to Prediction of Freezing Fronts in Soil, *Cold Regions Sci. Technol.*, vol. 6, pp. 115-121, 1982.
2. T. V. Hromadka II and G. L. Guymon, A Complex Variable Boundary Element thod, *Int. J. Numer. Methods Eng.*, in press.
3. J. W. Dettman, *Applied Complex Variables*, Macmillan, New York, 1969.
4. O. C. Zienkiewicz, *The Finite Element Method*, McGraw-Hill, New York, 1977.

Received August 1, 1983
Accepted February 13, 1984

Requests for reprints should be sent to T. V. Hromadka II.